Leveraging Common User Clustering for Improved Performance in Cell-Free NOMA Networks

S. Ali Mousavi
Shiraz University of Technology
Mehdi Monemi
mehdi.monemi@oulu.fi

Salman Farsi University of Kazerun
Reza Mohseni
Shiraz University of Technology

Research Article

Keywords: Cell-free NOMA networks, UE clustering, AP grouping, power allocation, signomial programming

Posted Date: April 15th, 2024

DOI: https://doi.org/10.21203/rs.3.rs-4242541/v1

Additional Declarations: No competing interests reported.

Leveraging Common User Clustering for Improved Performance in Cell-Free NOMA Networks

S. Ali Mousavi[1], Mehdi Monemi[2*], Reza Mohseni[3]

[1]Dept. Electrical Engineering, Shiraz University of Technology, Shiraz, Iran.

[2*]Dept. Electrical Engineering, Salman Farsi University of Kazerun, Kazerun, Iran.

[3]Dept. Electrical Engineering, Shiraz University of Technology, Shiraz, Iran.

*Corresponding author(s). E-mail(s): mehdi.monemi@oulu.fi;
Contributing authors: al.mousavi@sutech.ac.ir; mohseni@sutech.ac.ir;

Abstract

In existing cell-free non-orthogonal multiple access (NOMA) networks, each user equipment (UE) receives desired signals from a group of access points (APs) simultaneously, however, the UE belongs to only a single NOMA cluster. This prevents exploiting the potential benefits of having clusters with common UEs. Previous studies have investigated clusters with common UE in cellular NOMA networks by considering that UEs at the cell borders can communicate with base stations through multiple clusters using coordinate multi-point techniques. However, this approach has not been investigated for cell-free NOMA networks yet. In this paper, we consider the UE clustering in a cell-free NOMA network considering three strategies, including single-UE OMA (CF-OMA), double-UE NOMA with no common UE (CF-NOMA), and double-UE NOMA with common UE (CF-NOMAC) clusters. We analytically prove that the proposed CF-NOMAC clustering improves the sum rate compared to the CF-NOMA, and CF-OMA methods, provided that certain conditions hold. Considering the three characterized UE clustering methods, we formally define UE clustering, AP grouping, and power allocation problem for maximizing the sum rate in cell-free NOMA networks. We decompose the formulated mixed-integer non-linear program (MINLP) problem into subproblems with integers and continuous decision variables. The integer decision variables correspond to UE clustering and AP grouping which are obtained based on the analytically elaborated results, and the continuous ones correspond to the power values that are obtained by converting a non-convex

signomial programming problem into geometrical programming using the monomial approximation technique. Analytical results reveal the outperformance of the proposed algorithm due to employing a lower number of orthogonal clusters in the network.

Keywords: Cell-free NOMA networks, UE clustering, AP grouping, power allocation, signomial programming

1 Introduction

Spectrum is a valuable and limited resource in the highly demanded next-generation wireless networks. Two key enabling technologies (KET) for achieving high spectral efficiency (SE) in the sixth generation of wireless networks (6G) are cell-free networks and non-orthogonal multiple access (NOMA) techniques [1, 2]. Cell-free networks typically encompass multiple access points (APs) distributed in the network area, all connected to a central processing unit (CPU). This architecture offers numerous advantages. First, the use of distributed antennas enables cell-free networks to cover a large number of user equipments (UEs), ensuring extensive connectivity [3]. Furthermore, the distributed architecture of cell-free networks enables improved spatial reuse of the available spectrum, reducing interference and improving overall SE. On the other hand, the NOMA technique can also enhance SE. Unlike orthogonal multiple access (OMA), which assigns orthogonal spectrum to each UE, NOMA allows multiple UEs to share the same time-frequency resources by allocating different power levels to each UE [4], [5]. This enables simultaneous transmissions in a common bandwidth and enhances network capacity. In the downlink NOMA, the UEs characterized by stronger channel gains receive signals with lower power compared to the UEs with weaker channel gains. Strong UEs employ successive interference cancellation (SIC) techniques to alleviate the interference caused by stronger signals (relating to weaker UEs) in the same cluster. This interference cancellation process effectively improves the overall system capacity and performance. In recent years, extensive research has been carried out on the advantages presented by the integration of both cell-free and NOMA technologies. This has resulted in the attainment of higher data rates and increased coverage for a greater number of UEs [6-11]. These investigations have focused on various aspects such as AP selection strategies [7] and power allocation [8], as well as studying the SE maximization [9] in cell-free NOMA networks. In cell-free NOMA networks, UEs are categorized into separate clusters, where the signals transmitted within each cluster are generally designed to be orthogonal to those in other clusters. The implementation of dynamic OMA/NOMA switching methods can significantly enhance the performance in cell-free NOMA networks [10, 11]. In cellular NOMA networks, a noticeable difference in channel gain among UEs is desirable for classifying them into double-UE clusters. However, since there is no cell edge and all clusters can receive signals from all APs, a significant difference between UEs' channel gain may not be as crucial in cell-free NOMA networks [11].

Resource allocation (RA) techniques based on the NOMA method have been extensively studied in numerous papers, such as [2, 4]. In the case of cellular networks, a crucial issue is to efficiently cover the UEs located at the border of the cells. In cellular-NOMA networks, *coordinate multi-point* methods are employed to mitigate the interference for cell border UEs [12], [13], [14]. These methods encompass dynamic point selection (DPS), coordinated scheduling (CS), and joint transmission (JT) techniques as means to improve system performance [13]. The DPS technique entails continuously monitoring the channel state information (CSI) between the border UE and the base station (BS) in each cell. This enables the selection of the BS with the strongest channel quality to establish communication with the UE. In the CS technique, neighboring cells employ orthogonal signaling, which prevents potential interference experienced on the border UEs [13]. The JT technique requires that UEs receive signals from all adjacent cells, which, in turn, necessitates synchronous transmission of the same information from the BSs to border UEs [15], [16], [17]. Cell-free networks have emerged as a promising technology for wireless communication systems [1]. The addition of NOMA to cell-free networks can further enhance the system's SE, increase the number of simultaneously served UEs, and improve UE fairness [6]. In a conventional cell-free NOMA network, each **cluster** of NOMA UEs consists of multiple UEs being served by a **group** of APs, however, each UE is assigned to only a single cluster [18]. The issue of power allocation in cell-free NOMA networks is an important issue that highly affects the performance of the network. This has been extensively discussed in the literature [19], [20], [21]. The optimal solution of power allocation can be achieved through various criteria. Notably, the Max-min rate and sum rate are considered the most crucial criteria. The solution to power allocation in cell-free NOMA networks, employing the Max-min rate criteria, has been addressed in [11],[19], while the approach based on sum rate criteria has been resolved in [20], [21]. In [19], A closed-form SINR expression is derived under Rayleigh fading and used to formulate a max-min quality-of-service power control problem. In [20] sum-rate maximization problem is formulated for jointly optimizing the power allocation of the NOMA downlink, the uplink transmit power, and both the beamformer of the satellite and of the APs. Additionally, the analysis of UE clustering in cell-free NOMA networks holds substantial importance. In [22] two methods of UE clustering are proposed based on the similarity of large-scale fading coefficients, which are named UE similarity combination algorithm and mean shift clustering algorithm. The authors of [23] develop two efficient unsupervised machine learning-based UE clustering algorithms, namely k-means++ and improved k-means++, to effectively cluster UEs into disjoint clusters in a cell-free NOMA massive MIMO network. The authors of [24] investigated the necessity for optimizing UE clustering to maximize the benefits of NOMA for a cell-free network, emphasizing the importance of efficient clustering, and then proposed an optimal UE pairing strategy to group UEs that jointly optimizes the minimum downlink rate per UE and power allocation at an acceptable cost of complexity.

It is worth noting that all the previous studies have focused on independent NOMA clusters, where no UE is shared between them. While RA with common-UE clustering has been explored in cellular NOMA networks, the advantages of power allocation and AP grouping under efficient UE clustering in cell-free NOMA networks, where clusters

may or may not have common UEs, have not been investigated in the literature to date.

The main contributions of this work are expressed as follows:

- We consider a downlink NOMA/OMA cell-free network consisting of AP groups as well as different types of UEs' clusters, including single-UE OMA (simply denoted by CF-OMA), double-UE NOMA with no common UE (CF-NOMA), and double-UE NOMA with common UE (CF-NOMAC) clusters. We consider that each UE of a *cluster* can receive signals from a *group* of APs within its coverage area. Till now, cellular NOMA networks with common UE clusters have been dealt with in the literature in several works, wherein common UEs are assumed to be located near the cell borders; however, to the best of our knowledge, RA for NOMAC clusters has not been investigated in the literature for cell-free NOMA networks so far. In general, handling RA problems for NOMAC clusters in cell-free networks is more challenging compared to those in cellular networks. We formally define a novel sum rate optimization problem with UE clustering, AP grouping, and power allocation in a cell-free NOMA network considering the three CF-OMA, CF-NOMA, and CF-NOMAC cluster types.
- We decompose the proposed mixed integer non-linear program (MINLP) problem into integer programming and continuous subproblems, where the former relates to the UE clustering and AP grouping, and the latter deals with the allocation of the power levels. For discrete decision variables, first, we analytically compare the three clustering methods and prove that the proposed CF-NOMAC clustering method outperforms others in terms of sum rate, provided that certain conditions hold. Therefore, we consider the UE clustering to enhance the system's overall performance by exploiting the benefits of common UE clusters. In this regard, the priority is to consider as many CF-NOMAC clusters as possible, provided that corresponding constraints hold. Meanwhile, AP grouping aims at optimally assigning the resources of the APs to the UEs of each cluster, considering the limited set of APs in the coverage area of each UE. Based on these objectives, we propose novel algorithms for UE clustering and AP grouping that solve the integer part of the original optimization problem.
- The power allocation corresponding to sum rate optimization has been discussed in numerous works for cellular and/or NOMA networks. In cell-free NOMA networks, however, this problem has less been dealt with compared to the common max-min SE criterion considered for cell-free NOMA networks. To solve the power allocation sub-problem, we use the geometrical programming (GP) method. First, we show that the objective and constraints consist of a set of signomial expressions. Then, we apply the monomial approximation technique as a condensation method to approximate signomial expressions with suitable monomials. The effectiveness of the proposed solution schemes is verified in the numerical results.

The rest of the paper is organized as follows. The system model and problem formulation are expressed in Section II. In Section III, the proposed solution scheme for UE clustering, AP grouping, and power allocation is elaborated. Finally, numerical results and conclusions are presented in Sections IV and V respectively.

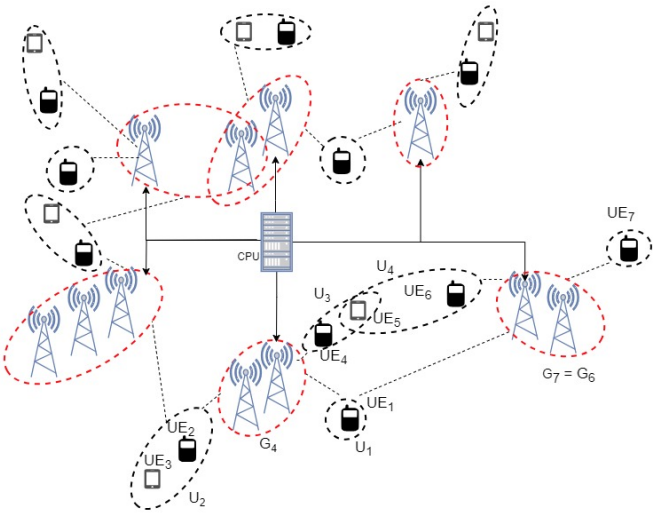

Fig. 1 The system model for cell-free NOMA network showing groups of APs in dashed red color, clusters of UEs in dashed black color, and a synchronizing CPU. APs are connected to the CPU in the cell-free network and UEs are divided into three types of clusters. UE1 belongs to a CF-OMA cluster, UE2 and UE3 belong to a CF-NOMA cluster, and finally, UE4, UE5, and UE_6 belong to the CF-NOMAC clusters.

2 System Model and Problem Formulation

2.1 System Model

We study a downlink cell-free NOMA network where a set of K UEs denoted by $\mathcal{K} = \{1, 2, ..., K\}$ are served by a set of N APs denoted by $\mathcal{N} = \{1, 2, .., N\}$, where the APs are coordinated by a CPU. Each AP is equipped with multiple RF chains and a set of N^D directional antennas to span the whole angular domain coverage. We assume that UEs are randomly distributed in the network and each UE has at least one serving AP in its vicinity. The UEs are divided into a set of clusters denoted by $\mathcal{C}$, where $\mathcal{C} = \mathcal{C}^O \cup \mathcal{C}^N \cup \mathcal{C}^{NC}$, in which $\mathcal{C}^O$, $\mathcal{C}^N$, and $\mathcal{C}^{NC}$ denote the set of CF-OMA, CF-NOMA, and CF-NOMAC clusters respectively. Fig.1 depicts such clusters in the cell-free NOMA network. Each CF-NOMA cluster is composed of two UEs where none is a member of any other clusters. However, as seen in the figure, for each CF-NOMAC cluster in the network, another CF-NOMAC cluster exists, with one common UE in both clusters. To prevent interference between signals transmitted to different clusters, we employ Orthogonal Frequency Division Multiplexing (OFDM). This technique allows us to divide the network's total bandwidth B into carriers that can be allocated to individual clusters without causing signal overlap. To optimize system performance and minimize complexity, we have set a limit of two UEs per CF-NOMA cluster, since increasing the number of UEs beyond two does not significantly improve the performance and adds more complexity to the system [4]. The cell-free network enables the UEs of each cluster to receive signals from multiple APs synchronously. The signal transmitted to each UE k is represented by x_k where $\|x_k\|^2 = 1$. Let p_{kn} denote the power transmitted

from AP n toward UE k, where the aggregate power of UEs from each AP is limited to P^{max}. The group of APs that transmit a signal to UE k, is denoted by G_k which is expressed in the following:

$$G_k = \{n \in \mathcal{N} | \beta_{kn} = 1\} \tag{1}$$

where β_{kn} is a binary parameter that indicates whether AP n transmits signal to UE k. The maximum allowed number of APs that can service each UE is denoted by N^{max}. The group of UEs assigned to each cluster c is denoted by U_c as expressed in the following:

$$U_c = \{k \in \mathcal{K} | \zeta_{kc} = 1\} \tag{2}$$

where ζ_{kc} is a binary parameter indicating whether UE k is a member of cluster c. Each U_c contains one UE if it is OMA type, or two UEs if it is NOMA or NOMAC type. The channel between UE k and AP n is denoted by $\hat{h}_{kn}$ which is modeled as $\hat{h}_{kn} = \xi_{kn}\sqrt{\kappa_{kn}}$ where $\xi_{kn} \sim CN(0,1)$ represents the small-scale fading and κ_{kn} represents the large-scale fading (LSF) [25] which is modeled as $\kappa_{kn} = PL_{kn}.10^{\frac{\sigma_{sh}.z_{mk}}{10}}$ where PL_{kn} is the path-loss obtained as

$$PL_{kn} = \begin{cases} -L - 35\log_{10} d_{kn} & d_{kn} \geq \overline{d} \\ -L - 15\log_{10} \overline{d} - 20\log_{10} d_{kn} & \underline{d} < d_{kn} < \overline{d} \\ -L - 15\log_{10} \overline{d} - 20\log_{10} \underline{d} & d_{kn} \leq \underline{d} \end{cases} \tag{3}$$

and $10^{\frac{\sigma_{sh}.z_{mk}}{10}}$ represents the shadow fading with the standard deviation σ_{sh} equal to 8dB, $z_{mk} \sim N(0,1)$, and $\overline{d}$ and $\underline{d}$ are determined distances, and

$$\begin{aligned} L = 46.3 \ + \ 33.9\log_{10} f \ - \ 13.82\log_{10} h_{AP} \\ - (1.1\log_{10} f \ - 0.7)\ h_{UE} + 1.56\log_{10} f - 0.8 \end{aligned} \tag{4}$$

In (4), h_{AP} and h_{UE} are AP's and UE's height, f is carrier frequency in MHz, and d_{kn} indicates the distance between UE k and AP n. In what follows, we represent the received signal and SINR for each of the three aforementioned clustering scenarios.

1) CF-OMA clusters: For each $c \in \mathcal{C}^O$, let U_c^O denote the UE of the CF-OMA cluster c. The signal received by UE k is obtained as follows:

$$y_k = \sum_{n \in G_k} \hat{h}_{kn}\sqrt{p_{kn}}x_k + \nu_k, \qquad k \in U_c^O \tag{5}$$

where $\nu_k \sim CN(0, N_0)$ represents the noise in which $N_0 = K'TBN^F$ is the noise power, K' is Boltzmann constant, T is temperature and N^F is noise figure. Note that p_{kn} is non-zero only for APs servicing UE k. The SINR received by UE k is obtained

as follows.

$$\gamma_k^O = \frac{\sum_{n\in G_k} h_{kn}^2 p_{kn}}{N_0}, \qquad k \in U_c^O \tag{6}$$

where $h_{kn} = |\hat{h}_{kn}|$.

2) CF-NOMA clusters: For each $c \in \mathcal{C}^N$, let U_c^N denote the set of UEs in the CF-NOMA cluster c. To make notations more simple, we consider $U_c^N = \{1, 2\}$, where UEs 1 and 2 are, respectively, strong and weak UEs. We simply consider that the following inequality holds for strong and weak UEs.

$$\sum_{n\in G_1} h_{1n}^2 \geq \sum_{n\in G_2} h_{2n}^2 \tag{7}$$

The signal received by UE $k \in \{1, 2\}$ is obtained as follows:

$$y_k = \sum_{\tilde{k}=1}^{2} \sum_{n\in G_{\tilde{k}}} \hat{h}_{kn} \sqrt{p_{\tilde{k}n}} x_{\tilde{k}} + \nu_k, \qquad k \in U_c^N \tag{8}$$

in which x_1 and x_2 are transmit signals relating to the strong and weak UEs respectively. Considering the basics of NOMA, a weaker power is allocated to the stronger UE, i.e. $\sum_{n\in G_2} p_{2n} > \sum_{n\in G_1} p_{1n}$. Hence, the stronger UE has to perform SIC to decode its signal by subtracting the weaker UE's signal, however, the weak UE can not remove the signal of the strong UE through SIC. Therefore, assuming perfect SIC for the strong UE, the SINRs of strong and weak UEs in the cell-free NOMA network are respectively expressed as follows:

$$\gamma_1^N = \frac{\sum_{n\in G_1} h_{1n}^2 \; p_{1n}}{N_0}, \qquad \gamma_2^N = \frac{\sum_{n\in G_2} h_{2n}^2 \; p_{2n}}{\sum_{n\in G_1} h_{2n}^2 \; p_{1n} + N_0} \tag{9}$$

3) CF-NOMAC clusters: Let $c \in \mathcal{C}^{NC}$, and $c' \in \mathcal{C}^{NC}$ be two CF-NOMAC clusters having one common UE. Let U_c^{NC} and $U_{c'}^{NC}$ denote the UEs of two NOMA clusters having three UEs with one common UE, as seen in Fig. 2. For simplicity, we have considered $U_c^{NC} = \{1, 2\}$ and $U_{c'}^{NC} = \{3, 2\}$, where UE_1 and UE_3 are the strong UEs of the corresponding clusters, and UE_2 is the weak common UE. The two clusters are assumed to share the same bandwidth. The APs are categorized into two distinct groups. The first group denoted by G_1 comprises the APs transmitting signals exclusively to the UEs of the first cluster (i.e. UE_1 and UE_2). Similarly, the APs in G_3 transmit the signal to exclusively to the UEs in the second cluster (i.e. UE_3 and UE_2).

$$h_{1n'} \gg h_{1n''} \tag{10a}$$
$$h_{1n'} > h_{2n'} \tag{10b}$$
$$h_{3n''} \gg h_{3n'} \tag{10c}$$
$$h_{3n''} > h_{2n''} \tag{10d}$$

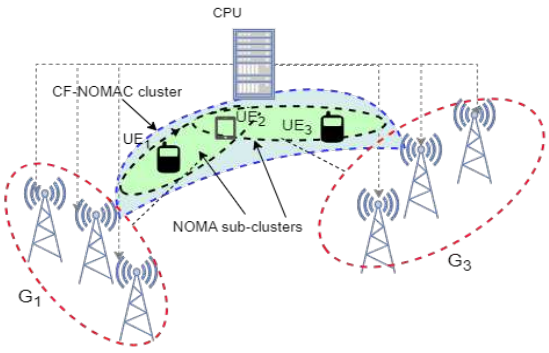

Fig. 2 Two groups of APs serving two CF-NOMAC clusters. UE2 is the common user.

$$\forall n' \in G_1, \forall n'' \in G_3$$

Remark 1. *To guarantee the feasibility of the SIC, constraint* (10) *should hold. It should be noted that in practice, the UEs are distributed randomly all over the network area. Therefore, as will be explained later, the UE clustering is achieved in a way that proper UEs are grouped as clusters such that this condition holds for as many clusters as possible considering a rather dense distribution of UEs, it is of probability that there exist numerous UEs for which the constraint* (10) *is satisfied.*

The signal received by UE $k \in \{1, 2, 3\}$ is obtained as follows:

$$y_k = \sum_{\tilde{k}=1}^{3} \sum_{n \in G_{\tilde{k}}} h_{kn} \sqrt{p_{\tilde{k}n}} x_{\tilde{k}} + \nu_k, \quad k \in \{1, 2, 3\} \tag{11}$$

where $p_{1n''} = p_{3n'} = 0, \forall n' \in G_1, n'' \in G_3$. Assuming perfect SIC for UE_1 and UE_3, the SINRs of the UEs are obtained as follows:

$$\begin{aligned}
\gamma_1^{NC} &= \frac{\sum_{n' \in G_1} h_{1n'}^2 \; p_{1n'}}{N_0} \\
\gamma_2^{NC} &= \frac{\sum_{n \in G_1 \cup G_3} h_{2n}^2 \; p_{2n}}{\sum_{n' \in G_1} h_{2n'}^2 \; p_{1n'} + \sum_{n'' \in G_3} h_{2n''}^2 \; p_{3n''} + N_0} \\
\gamma_3^{NC} &= \frac{\sum_{n'' \in G_3} h_{3n''}^2 \; p_{3n''}}{N_0}
\end{aligned} \tag{12}$$

In the following, we may use the notation γ_k to stand for any of the SINRs γ_k^O, γ_k^N, or γ_k^{NC}, and notation U_c to stand for any of cluster UEs U_c^O, U_c^N, or U_c^{NC}.

2.2 Problem Formulation

Based on what stated so far, given the set of UEs and APs in a cell-free NOMA network, we aim to maximize the sum rate by optimally clustering the UEs, grouping the

APs, and allocating the downlink transmit powers, considering all relating constraints hold. This is formally defined as follows.

$$\max_{p_{kn},\beta_{kn},\zeta_{kc},\mu_k} \quad \sum_k \{u(\mu_k - 1)\log(1+\gamma_k^O) + u(-|\mu_k|)\log(1+\gamma_k^N) + u(-\mu_k - 1)\log(1+\gamma_k^{NC})\} \tag{13}$$

$$\text{s.t.} \quad C1 : \sum_k p_{kn} \leq P^{max},\ \forall n \in \mathcal{N}$$

$$C2 : p_{k''n} - p_{k'n} \geq \frac{P^{tol} N_0}{h_{k''n}},\ \forall c \in \mathcal{C}^N \cup \mathcal{C}^{NC},\ k', k'' \in U_c^N \text{ OR } k', k'' \in U_c^{NC}$$

$$C3 : \log(1+\gamma_k) \geq R^{min}, \quad \forall k \in \mathcal{K}$$

$$C4 : \sum_{n \in G_k} \beta_{kn} \leq N^{max}, \qquad \forall k \in \mathcal{K}$$

$$C5 : 1 \leq \sum_k \zeta_{kc} \leq 2, \quad \forall c \in \mathcal{C}$$

$$C6 : U_c^O \cap U_{c'}^O = \emptyset, \qquad \forall c \neq c' \in \mathcal{C}^O$$

$$U_c^N \cap U_{c'}^N = \emptyset, \qquad \forall c \neq c' \in \mathcal{C}^N$$

$$|U_c^{NC} \cap U_{c'}^{NC}| = 1, \quad \forall c \neq c' \in \mathcal{C}^{NC}$$

$$C7 : \mu_k \in \{-1, 0, 1\},\ \beta_{kn} \in \{0, 1\},\ \zeta_{kc} \in \{0, 1\},\ \forall k \in \mathcal{K}, n \in \mathcal{N}, c \in \mathcal{C}$$

where μ_k represents the cluster type of UE k. If UE k is a member of CF-OMA, CF-NOMA, or CF-NOMAC clusters, μ_k is 1, 0, or -1 respectively, and $u(.)$ is the unit step function expressed as follows:

$$u(x) = \begin{cases} 1 & x \geq 0 \\ 0 & x < 0 \end{cases} \tag{14}$$

In (**??**), $C1$ ensures that the maximum downlink transmit power of each AP n is limited to the allowed threshold P^{max}, and $C2$ guarantees the feasibility of SIC, where P^{tol} is the minimum power difference required for implementing SIC in CF-NOMA and CF-NOMAC clusters.

$C3$ guarantees that the achieved rate of each UE k is higher than the minimum desired value R^{min}. $C4$ specifies that the number of APs in each group is limited to N^{max}, and $C5$ states that the number of UEs in each cluster is limited to 1 for OMA and 2 for NOMA and NOMAC clusters. $C6$ ensures that there exists no common UE in OMA and NOMA clusters, and one common UE in NOMAC clusters, and finally $C7$ specifies the sets of valid values for the decision variables.

3 Proposed Solution Scheme

In order to handle the NP-Hard problem expressed in (**??**), we split the stated problem into three sub-problems namely UE clustering, AP grouping, and power allocation.

We investigate each sub-problem separately in order to obtain the overall resource management algorithm.

3.1 UE clustering

In this part, we will analyze the UE clustering process. This process enable us to obtain the parameters ζ_{kc} and β_{kn} for all $k \in \mathcal{K}$, $n \in \mathcal{N}$, and $c \in \mathcal{C}$. The contribution of UE clustering and AP grouping is derived by jointly considering the parameter β_{kn}. We hereby present two theorems that constitute the optimal metrics for UE clustering and AP grouping. More specifically, we formally analyze the benefits of CF-NOMAC over CF-NOMA and CF-OMA clustering methods. By using CF-NOMAC clustering, the network can improve the sum rate by allocating the bandwidth more effectively to the UEs and reducing the number of orthogonal clusters needed to serve all UEs. Although the UE clustering algorithm pertains to the entire UEs of the network, first, we consider the clustering problem for the simple case of a set of 3 UEs and then extend the results for the general case considering all UEs of the network. Consider the set of three UEs denoted by $\{1, 2, 3\}$, operating in a cell-free network with two groups of serving APs, denoted by G_1 and G_3, where UEs can be clustered in one of the following three scenarios: **CF-OMA** where all UEs employ OMA each allocated one-third of the available bandwidth, **CF-NOMA**, where one of the UEs operates as an OMA cluster (we consider UE 3 as OMA cluster) and the two remaining operate as a NOMA cluster, and each cluster occupies one-half of the spectrum, and finally **CF-NOMAC**, where three UEs operate as two NOMA clusters with a common UE (we consider UE 2 as common UE), and each cluster is allocated the whole spectrum. In the following, we first provide the conditions under which CF-NOMA outperforms CF-OMA, and then show how CF-NOMAC outperforms the other schemes under certain conditions.

Theorem 1. *In cell-free NOMA networks, the CF-NOMA cluster outperforms CF-OMA in terms of sum rate under high-SNR conditions for each UE, if the following inequality holds.*

$$\frac{h_{1n'}h_{3n''}}{h_{2n'}^2 + h_{2n''}^2} \geq 3/2$$
$$\forall n' \in G_1, \forall n'' \in G_3 \tag{15}$$

Proof. See **Appendix I**.

Theorem 2. *In cell-free NOMA networks, the NOMAC clustering outperforms NOMA in terms of sum rate under high-SNR conditions.*

Proof. See **Appendix I**.

Remark 2. *Constraint (15) is a sufficient (and not necessary) condition for the outperformance of CF-NOMA over CF-OMA in cell-free networks. On the other hand, by considering that the constraints in (10) hold, one can verify that (15) is verified most of the time in practice.*

Remark 3. *The superior performance of CF-NOMA compared to CF-OMA can be attributed to its higher bandwidth allocation for CF-NOMA UEs, which effectively mitigates the detrimental impact of interference generated by the NOMA technique.*

Similarly, CF-NOMAC outperforms CF-NOMA due to the higher bandwidth allocation provided to CF-NOMAC UEs.

Remark 4. *Based on the expressed theorems, CF-NOMAC clustering improves cell-free NOMA network performance. Therefore, the priority is to include as many UEs as possible in these clusters. The next priorities are to place UEs in CF-NOMA clusters and finally CF-OMA clusters. Although the outperformance of CF-NOMAC in Theorem 2 is stated for high SNR regimes, we will validate the superiority of that for various SNRs through numerical results.*

The UE clustering algorithm has two steps as follows:

I) Selection of the first UE of each cluster

In the initial phase, for each AP n, we consider a new cluster c with a single UE which is selected as the UE corresponding to the strongest available channel. Therefore, we have

$$k_c^1 = \underset{k \in \mathcal{K}}{\operatorname{argmax}}\ h_{kn}, \quad \forall n \in \mathcal{N} \tag{16}$$

where k_c^1 is the first member of the set of UEs associated with one direction of AP n through cluster c. Consequently, we set $\zeta_{k_c^1 c} = 1$, $\beta_{k_c^1 n} = 1$, and $U_c = \{k_c^1\}$. We construct the set of first UEs of all clusters as follows:

$$Q^1 = \{k_c^1\}, \quad \forall c \in \mathcal{C} \tag{17}$$

II) Selection of the second UE

The NOMA method experiences a decline in performance when the channels between UEs within the same cluster and the corresponding APs are close to each other. To mitigate this issue, the clustering algorithm mandates that UEs within a cluster must be separated by a distance greater than a predefined threshold, denoted as d^{min}. Consider k_c^2 is the second member of the set of UEs associated with AP n through cluster c. We define the set Q_c^2 to encompass all second UE candidates that may be associated with cluster c, which is organized as follows:

$$Q_c^2 = \{k \notin Q^1 | \underbrace{d^{min} < d_{k_c^1 n} - d_{kn}}_{A}, \underbrace{|\Delta\phi_{k_c^1,k}| < \phi^{th}}_{B}\} \tag{18}$$

From the set of all UEs except the ones in Q^1, we search through those located in the main lobe of the beam forwarded to the first UE (k_c^1), and the distance difference between k_c^1 and other potential candidates with respect to AP n be higher than d^{min}. This is expressed as the SIC constraint in term A of (18). Considering that AP n steers the beam (with maximum directivity) toward the first UE, term B of (18) ensures that the relative phase angle between (AP n, UE k_c^1) and (AP n, UE k_c^2) denoted by $|\Delta\phi_{k_c^1,k}|$ is smaller than a threshold value ϕ^{th}. This ensures that the first (near) and second (far) UEs are aligned to a desired extent.

Once the first UE and second UE candidates for all clusters are processed according to the above procedure, we choose the clusters' types as follows. For each $c \in \mathcal{C}$, if Q_c^2 is null (i.e. there exists no UE for which constraints A and B hold), cluster c

Algorithm 1 : UE clustering

Initialize: Set $\zeta_{kc} = 0, \quad c = n,\ \beta_{kn} = 0 \quad \forall k, n;$
for each c **do**
  Select UE k_c^1 from (16);
  Set $\zeta_{k_c^1 c} = 1;$
end for
Construct Q^1 and Q_c^2 from (17) and (18);
for each c **do**
  if $|Q_c^2| = 0$ **then**
    Determine the clustering type of c as CF-OMA and $\mu_{k_c^1} = 1;$
  else if $|Q_c^2| \neq 0, \quad |Q_c^2 \cap Q_c^2| = 0,\ \forall c \neq c'$ **then**
    Select UE k_c^2 from (19);
    Set $\zeta_{k_c^2 c} = 1;$
    Determine the clustering type of c as CF-NOMA and $\mu_{k_c^1} = \mu_{k_c^2} = 0;$
  else if $|Q_c^2| \neq 0,\ |Q_c^2 \cap Q_c^2| \neq 0,\ \forall c \neq c'$ **then**
    Select UE k_c^2 from (20);
    Set $\zeta_{k_c^2 c} = \zeta_{k_c^2 c'} = 1;$
    Determine the clustering type of c, c' as CF-NOMAC and $\mu_{k_c^1} = \mu_{k_{c'}^1} = \mu_{k_c^2} = -1;$
  end if
end for

corresponding to UE k_c^1 is selected as a single UE CF-OMA ($U_c^{OMA} = \{k_c^1\}$). In order to handle the CF-NOMA and CF-NOMAC clusters, we note that the sets $Q_c^2,\ \forall c$ may or may not intersect with each other. In the case that there exists no common UE between Q_c^2, and $Q_{c'}^2,\ \forall c' \neq c$ (i.e. $Q_c^2 \cap Q_{c'}^2 = \emptyset,\ \forall c \neq c'$), we assign the second UE of cluster c denoted by k_c^2 from the set of candidate UEs Q_c^2 , where k_c^2 is obtained from (19) and cluster c (containing UEs k_c^1 and k_c^2) is labeled as CF-NOMA ($U_c^{NOMA} = \{k_c^1,\ k_c^2\}$).

$$k_c^2 = \underset{k \in Q_c^2}{\operatorname{argmax}}\ h_{kn}, \quad \forall c \in \mathcal{C} \tag{19}$$

Consequently, we set $\zeta_{k_c^2 c} = 1$ and $\beta_{k_c^2 n} = 1$. If Q_c^2 has a common UE with $Q_{c'}^2$ for some $c' \neq c$ (i.e. $|Q_c^2 \cap Q_{c'}^2| \neq 0,\ \forall c' \neq c$), k_c^1, k_c^2 and $k_{c'}^1$ form CF-NOMAC clusters as $U_c^{NC} = \{k_c^1,\ k_c^2\}$ and $U_{c'}^{NC} = \{k_{c'}^1,\ k_{c'}^2\}$, where $k_{c'}^2 = \ k_c^2$ is obtained as follows:

$$k_c^2 = \underset{k \in Q_c^2 \cap Q_{c'}^2}{\operatorname{argmax}}\ (1 + \gamma_{k_c^1}^{NC})(1 + \gamma_{k_c^2}^{NC})(1 + \gamma_{k_{c'}^1}^{NC}), \quad \forall c, c' \in \mathcal{C} \tag{20}$$

To address the optimization problem stated in equation (20), we employ Algorithm 3 which is detailed in the subsequent two subsections. Consequently $\zeta_{k_c^2 c} = 1$, $\beta_{k_c^2 n} = 1$, $\zeta_{k_c^2 c'} = 1$ and $\beta_{k_c^2 n'} = 1$ where n' is the AP initially associated with cluster c'. We repeat the above steps until all UEs are clustered. Based on what is stated so far, the proposed UE clustering is presented in Algorithm 1.

Algorithm 2: AP Grouping Algorithm

Initialization: Let ζ_{kc} be known from the clustering scheme presented in Algorithm 1;
for each $k \in \mathcal{K}$ **do**
  Construct Q_k^{AP} from (21);
  if $\mu_k \in \{0, 1\}$ **then**
    Select the first $\min\{N^{max} - 1, |Q_k^{AP}|\}$ elements of Q_k^{AP} and set $\beta_{kn} = 1$ for these decision variable;
  else if μ_k=-1 **then**
    if $k = k_c^1$ **then**
      Update Q_k^{AP} by applying constraints (10);
    else if $k = k_c^2$ **then**
      Update Q_k^{AP} by applying constraints (10b) and (10d);
    end if
    Select the first $\min\{N^{max} - 2, |Q_k^{AP}|\}$ elements of Q_k^{AP} and set $\beta_{kn} = 1$ for these decision variable;
  end if
end for

3.2 AP grouping

From UE clustering each UE is assigned to 1 AP (for CF-OMA and CF-NOMA clusters, as well as the strong UE of CF-NOMAC clusters) or 2 APs (for weak common UE in the CF-NOMAC clusters). In cell-free networks, a set of multiple APs can simultaneously cover each UE to increase SE. We define the set Q_k^{AP} to include the APs capable of covering UE k as follows:

$$Q_k^{AP} = \{n \in \mathcal{N} | d_{kn} < D\}, \quad \forall k \in \mathcal{K} \tag{21}$$

where D is the maximum allowed distance between the UE and the AP candidate. For each UE k, we sort the members of Q_k^{AP} in descending order based on the h_{kn}, $\forall n \in Q_k^{AP}$. For UEs that belong to CF-OMA or CF-NOMA clusters ($\mu_k \in \{1, 0\}$), it's evident that the first member of Q_k^{AP} is the initial AP that covers UE k; We select the first $\min\{N^{max} - 1, |Q_k^{AP}|\}$ elements of Q_k^{AP} (excluding the initial AP) as addition APs that cover UE k. For UEs that belong to CF-NOMAC clusters ($\mu_k = -1$), it is essential to apply the following constraints in addition to (21); for strong UEs ($k = k_c^1$) within the CF-NOMAC clusters, the constraint specified in (10) and for weak UEs ($k = k_c^2$), (10b) and (10d), should be followed. After updating Q_k^{AP} We select the first $\min\{N^{max} - 2, |Q_k^{AP}|\}$ elements of Q_k^{AP} (excluding those that cover UE k) along with the initial AP as APs that cover UE k. Throughout the execution of this algorithm, the values of β_{kn}, $\forall k, n$ have been updated. The proposed AP grouping is presented in Algorithm 2.

3.3 Power allocation

After clustering UEs and grouping APs, we compute the optimal downlink transmit power of the APs towards the UEs as follows. Given that the variables associated with UE clustering and AP grouping $(\beta_{kn}, \zeta_{kn}, \mu_k)$ are computed using Algorithms 1 and 2, the power allocation problem corresponding to (**??**) can be written as follows:

$$\max_{\boldsymbol{p}_{kn}} \sum_{k\in\mathcal{K}} \log_2(1+\gamma_k) \quad \text{s.t.} \quad C1, C2, C3 \tag{22}$$

where γ_k can be any of the three terms γ_k^O,γ_k^N and γ_k^{NC}. Problem (22) is equivalent to the following problem:

$$\min_{p_{kn}} \prod_k \frac{1}{(1+\gamma_k)} \quad \text{s.t.} \quad C1, C2, C3 \tag{23}$$

After some mathematical manipulations, (23) can be written as (24).

$$\min_{p_{kn}} \frac{\sum_{i=0}^{I} l_i \prod_{j,k,n} (p_{kn}^{a_i^{(j)}} \cdot N_0^{a_0^{(j)}})}{\sum_{i'=0}^{I'} l'_{i'} \prod_{j,k,n} (p_{kn}^{a_{i'}^{(j)}} \cdot N_0^{a_0^{(j)}})} \quad \text{s.t.} \quad C1, C2, C3 \tag{24}$$

where l_i, $l'_{i'}$, $a_i^{(j)}$ and $a_{i'}^{(j)}$ are constant coefficients derived through basic mathematical operations, and I, I' are integer numbers whose values are usually much less than $K \times N$. The objective function of (24) is a ratio whose numerator and denominator are posynomials which can be approximated to monomial expressions through the monomial approximation technique and then solved through GP method [26]. The preliminaries of the GP method related to solving the stated power allocation problem are briefly presented in Appendix II. As described in Appendix II, (24) belongs to the category of signomial programming (SP), also known as Complementary GP, and can be effectively addressed through the condensation method. To solve this equation, we apply monomial approximation to the denominator of (24). The steps of obtaining the optimal power allocation through the GP method are expressed in Algorithm 3. As outlined in Section III, clusters that are outside the coverage range of an AP cannot receive signals from that AP. Consequently, equation (24) can be decomposed into multiple independent problems, each of which can be addressed separately. This approach enhances simplicity and reduces the computational complexity associated with solving the power allocation problem.

Remark 5. *Constraint $C3$ has the potential to render problem(23) infeasible; To mitigate this problem, we employ the user removal technique; if problem (23) is determined to be infeasible, the cell-free NOMA network proceeds by removing weak UEs from the*

Algorithm 3 : Power Allocation Algorithm

Initialize: Let $m \leftarrow 1$, where m is the step number, ϵ be a small number, and let $\boldsymbol{p}^0$ be an initial feasible power vector;
Do
  Compute the posynomial corresponding to the denominator of (24) using $\boldsymbol{p}^{m-1}$;
  for each $i' \in \{0, 1, ..., I'\}$ **do**
    Compute $\alpha_{i'}^*(\boldsymbol{p}^{m-1})$ from (B19);
  end
  Condense the posynomial denominator of (24) into monomial form by applying the weights $\alpha_{i'}^*(\boldsymbol{p}^{m-1})$ in (B18);
  Obtain $\boldsymbol{p}^m$ by solving the resulting GP optimization problem using the interior-point method;
While $\|\boldsymbol{p}^m - \boldsymbol{p}^{m-1}\| \geq \epsilon$;

coverage set based on their total channel gain until feasibility is achieved. The total channel gain of UE k is defined as $h_k^{Tot} = \sum_{n \in Q_k^{AP}} \|h_{kn}\|^2$.

3.4 Computational complexity

To analyze the computational complexity of Algorithms 1, 2, and 3, we evaluate their performance under the worst-case scenario, wherein the network considers the maximum number of CF-NOMAC clusters. The computational complexity of Algorithm 1 and Algorithm 2 is determined to be $O(NK + K^2)$ and $O(NK)$ respectively. On the other hand, the complexity of calculating Algorithm 3 is of $O((KN)^{3.5}\log(1/\epsilon) + (NK)^2 + NK) \equiv O((KN)^{3.5}\log(1/\epsilon))$ where ϵ is achievable precision [27]. Consequently, when addressing the optimization problem presented in equation (**??**), the maximum complexity among Algorithms 1, 2, and 3 is $O((KN)^{3.5}\log(1/\epsilon))$.

4 NUMERICAL RESULTS and DISCUSSIONS

Table 1 Simulation parameters

parameter	value
f	1.9 GHz
B	20 MHz
N^F	9 dB
Antenna gain	15 dB
h_{AP}, h_{UE}	15 m, 1.65 m
$\bar{d}, \underline{d}, d^{min}$, D	50 m , 10 m , 5 m, 500 m
P^{tol}	10 mW
N^D	3

In this section, we present numerical results to verify analytical justifications and proposed algorithms. Consider a 2Km × 2Km network area wherein a set of K UEs and a set of N APs are randomly distributed in the network area where the values of K

and N will be specified in each simulation scenario. Unless explicitly stated otherwise, all simulation parameters considered are listed in Table I. The channels between UEs and APs are modeled as (3). Simulation results have been obtained using the Monte Carlo method by averaging from 500 independent iterations and utilizing the CVX toolbox. To verify the superiority of the proposed CF-NOMAC clustering over CF-

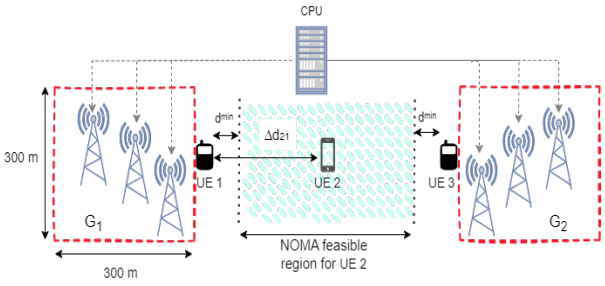

(a)

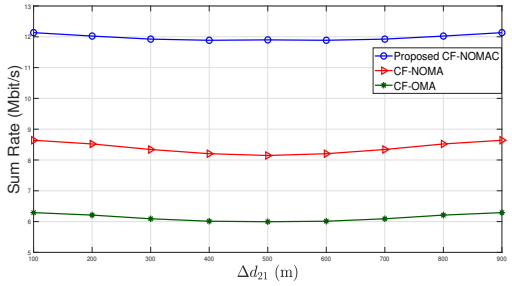

(b)

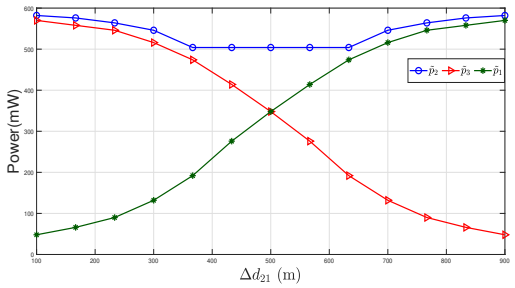

(c)

Fig. 3 (a) The scenario for analyzing the proposed clustering methods. Three UEs and two groups of APs with $P^{max} = 200$mW have been considered. UE1 and UE3 are assumed to be fixed, while UE2 moves within the feasible range. (b) Sum rate per Δd_{21} for three clustering methods. (c) Aggregate power of each UE per Δd_{21} for CF-NOMAC clustering method.

NOMA and CF-OMA methods, we have considered three UEs namely UE1, UE2, and UE3 according to Fig. 3-a communicating with two cell-free groups each consisting of

three APs with $P^{max} = 200mW$, where the location of each of the APs is randomly set in the corresponding dashed square region where UE1 and UE3 are assumed to be fixed, while UE2 can move within a predetermined range. The distance between UE1 and UE3 is considered to be 1 km. Fig.3-b illustrates the sum rate per Δd_{21}. As shown in the figure, the CF-NOMAC clustering method presented in this paper exhibits superior performance compared to the others. Increasing Δd_{21} from d^{min} to 500 results in a decrease in channel gains between UE2 and each of the APs of G_1, thereby resulting in a reduction in the sum rate. This, however, is not substantial due to UE2's proximity to the APs of the G_3 group. Due to the network symmetry, the sum rate continues to increase as Δd_{21} exceeds the 500-meter threshold. By allowing a UE to be jointly a member of the two clusters, even though the interference of signals of the two clusters has a destructive effect on the common UE, the number of orthogonal clusters is decreased which in turn can lead to a performance leverage. Fig.3-c depicts the aggregate downlink transmit power toward each UE k denoted by $\widetilde{p}_k$ ($k \in \{1, 2, 3\}$) per Δd_{21} for the network model presented in Fig.3-a. It is seen that increasing Δd_{21} results in a monotonic increase (decrease) in $\widetilde{p}_1$ ($\widetilde{p}_3$) with a relatively high rate, however, $\widetilde{p}_2$ is always greater than $\widetilde{p}_1$ and $\widetilde{p}_3$ to satisfy $C2$ in (**??**). Moreover, the variation of $\widetilde{p}_2$ is minimal due to the fact all APs of $G_1 \cup G_2$ contribute to $\widetilde{p}_2$, and besides, although increasing Δd_{21} results in less power to be allocated to UE2 from the APs of G_1, this is somehow compensated by assigning more power from the APs of G_3. In the following, we consider 4 RA algorithms to verify the performance of

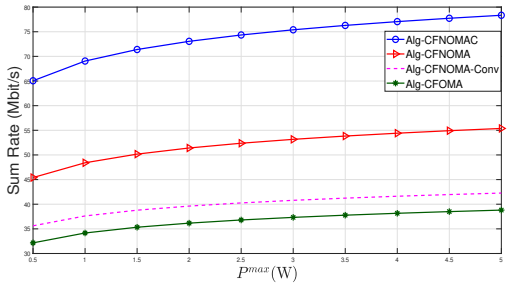

Fig. 4 Sum rate per P^{max}. The network has $K = 60$ UEs and $N = 20$ APs.

our proposed algorithm. In the first scenario, we consider that the UE clustering, AP grouping, and power allocation are obtained respectively from Algorithms 1, 2, and 3. We call this Alg-CFNOMAC. In the second scenario, we consider the case where clusters are exclusively determined by NOMA and OMA methods, and in the third scenario, we consider the pure OMA method. We call these Alg-CFNOMA and Alg-CFOMA respectively. Finally, we consider the NOMA clustering where UE pairs are selected. This is called Alg-CFNOMA-Conv.

Fig. 4 illustrates the sum rate of the UEs versus P^{max} in a network with $K = 60$ UEs and $N = 20$ APs. Firstly, it is observed how the sum rate increases with an increase in P^{max} for all stated algorithms. For example, for Alg-CFNOMAC, increasing P^{max} from 1 to 4 W, results in an increase from 69 Mbit/s to 79 Mbit/s, while the

power increase is rather substantial, the resulting performance leverage is not determinant. On the other hand, it is seen that Alg-CFNOMAC outperforms Alg-CFNOMA, and Alg-CFNOMA outperforms Alg-CFOMA to a great extent. For example, for $P^{max} = 1W$, the performance of Alg-CFNOMAC is higher than Alg-CFNOMA and Alg-CFOMA about 47% and 30% respectively. In a similar way, Fig. 5 illustrates how increasing the number of APs in the cell-free NOMA network improves the performance of the different RA algorithms. It is seen that the sum rate of our proposed algorithm is much higher than all other schemes for all values of the number of APs. This is related to more efficient channel diversity gain achieved through increasing the probability of accessing APs with higher channel gains. Both Fig. 4 and Fig. 5 illustrate that the proposed CF-NOMAC clustering method outperforms traditional clustering methods. Considering a fixed value for the number of APs as $N = 20$, Fig.

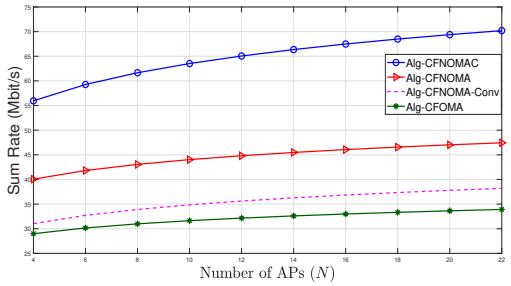

Fig. 5 Sum rate per number of APs (N). The network has $K = 60$ UEs.

6 illustrates how increasing the number of UEs (K) affects the sum rate of the network for two cases of $R^{min} = 0$ and $R^{min} = 0.25$ Mbit/s corresponding to Figs. 6-a and 6-b respectively. To take the limitations of channel estimation into account, similar to [25], we have considered that a pre-log-factor of $(1 - \frac{\tau}{\tau_{cf}})$ multiplied by the rate of each UE where τ represents the pilot sequence length which is always greater than or equal to the number of orthogonal clusters and τ_{cf} is coherence interval, where we have assumed $\tau_{cf} = 50$. For Alg-CFOMA, and Alg-CFNOMA-Conv, τ is equal to K and $K/2$ respectively. For Alg-CFNOMA which employs both CF-OMA and CF-NOMA clustering types, the value of τ always holds the inequality $\frac{K}{2} < \tau \leq K$. Similarly, for the Alg-CFNOMAC wherein the clusters might be either of CF-OMA, CF-NOMA, or CF-NOMAC types, we have $\frac{K}{3} < \tau \leq \frac{K}{2}$. Consequently, the upper bound for serving UEs for Alg-CFNOMAC and Alg-CFNOMA are up to twice and three times, respectively, compared to the Alg-CFOMA. As illustrated in both Figs. 6-a and 6-b, the maximum number of UEs that can be served in the Alg-CFNOMA and Alg-CFNOMAC are lower than 100 and 150, respectively. To justify this, note that due to the random distribution of UEs and APs, the constraints of (10) and (18) may not be satisfied for all UEs. Therefore, Alg-CFNOMA leads to the constitution of both CF-OMA and CF-NOMA clusters, and Alg-CFNOMAC constitutes all CF-OMA, CF-NOMA, and CF-NOMAC clusters. It is also seen that in both figures and for all values of K, Alg-CFNOMAC has the superior performance, however, the other

three algorithms show different performance behavior for different values of K. To analyze the behavior of these diagrams, we should note that the performance of each of the studied algorithms is tightly related to the two parameters of SINR and the number of orthogonal clusters. A higher level of sum rate is associated with higher SINRs and a smaller number of orthogonal clusters, while a wider diagram is associated with a smaller number of orthogonal clusters. The performance of Alg-CFOMA is mostly related to the first factor, while that of other algorithms is influenced by the two factors. It is seen that Alg-CFNOMAC has taken the benefits of both high SINR and the smaller number of orthogonal clusters. In contrast to Fig. 6-a wherein $R^{min} = 0$, the minimum rate of Fig.6-b, it is observed that the implementation of a minimum rate of $R^{min} > 0$ results in less number of supported UEs (due to the user removal mechanism), leading to service sustainability for the maximum possible number of UEs.

In order to show how the proposed Alg-CFNOMAC allocates different types of CF-NOMAC, CF-NOMA, and CF-OMA clusters to the UEs, the corresponding number of allocated clusters per number of UEs is depicted in Fig. 7. For a small number of UEs, it is of little probability to find UE pairs for which the constraints relating to CF-NOMA and CF-NOMAC hold. Therefore, in this case, as seen in the figure, most UEs are clustered as CF-OMA. This justifies the close performance measures of all algorithms for a small number of UEs. On the other hand, as the number of UEs increases, more UE candidates are available to be clustered as CF-NOMA and CF-NOMAC. This results in gaining higher efficiency of Alg-CFNOMAC for a larger number of UEs compared to other algorithms.

5 CONCLUSIONS

Our paper extensively presents and examines the performance advantages of a clustering method in cell-free NOMA networks that share a common UE between two clusters which we refer to as CF-NOMAC cluster. We provided mathematical proofs and numerical results to substantiate the superiority of CF-NOMAC over traditional clustering schemes like NOMA and OMA in cell-free networks. Additionally, we introduced UE clustering and AP grouping algorithms which efficiently decrease the number of orthogonal clusters. To efficiently address the power allocation problem, we utilized geometrical and signomial programming. Noting that the proposed solution schemes are inherently sub-optimal, in future works we anticipate significant potential in exploiting machine learning and artificial intelligence algorithms to optimize UE clustering, as well as AP grouping for cell-free NOMA networks employing CF-NOMAC clusters.

Appendix A PROOF OF THEOREMS I, II

A) Proof of Theorem I: In what follows, first, we provide the proof for the case where each cluster is serviced by only one AP, namely $n' \in G_1$ and $n'' \in G_3$; then we justify that the proof is valid for the general case of multiple APs servicing each UE in the cell-free network. The power allocation for maximizing the sum rate corresponding

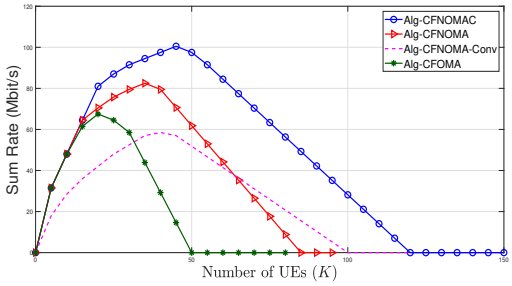

(a)

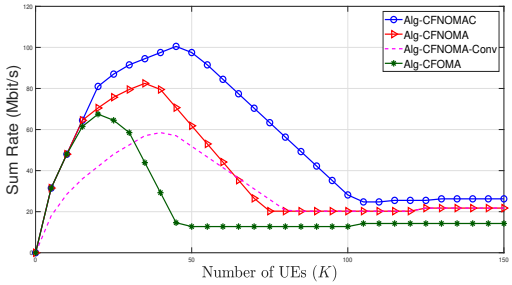

(b)

Fig. 6 Sum rate per number of UEs (K). The network has $N = 20$ APs: a) $R^{min} = 0$Mbit/s. b) $R^{min} = 0.25$Mbit/s.

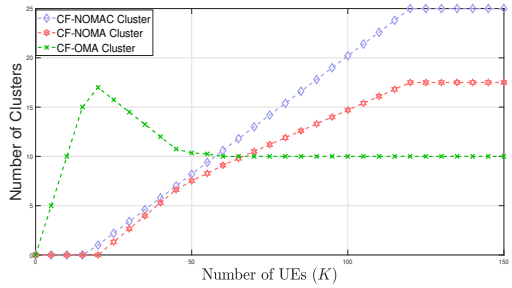

Fig. 7 Number of clusters per number of UEs (K) for Alg-CFNOMAC. The network has $N = 20$ APs and $\tau_{cf} = 50$.

to the CF-OMA clustering is obtained as (A1):

$$\max_{p_{1n'},p_{2n'},p_{2n''},p_{3n''}} \log_2\left(\left(1+\frac{h_{1n'}^2 p_{1n'}}{N_0}\right)\left(1+\frac{h_{2n'}^2 p_{2n'}+h_{2n''}^2 p_{2n''}}{N_0}\right)\left(1+\frac{h_{3n''}^2 p_{3n''}}{N_0}\right)\right)^{\eta}$$
$$\text{s.t.} \quad p_{1n'}+p_{2n'} \le P^{max}$$
$$p_{2n''}+p_{3n''} \le P^{max} \tag{A1}$$

where $\eta = B^{OMA}/B = 1/3$ and B^{OMA} is the allocated bandwidth to each UE of the CF-OMA cluster. Considering the high SNR assumption, (A1) is equal to (A2), expressed as follows.

$$\begin{aligned} \max_{p_{1n'}, p_{2n'}, p_{2n''}, p_{3n''}} \quad & f(\boldsymbol{p}) \\ \text{s.t.} \quad & p_{1n'} + p_{2n'} \leq P^{max} \\ & p_{2n''} + p_{3n''} \leq P^{max} \end{aligned} \tag{A2}$$

where

$$f(\boldsymbol{p}) = \left(\left(\frac{h_{1n'}^2 p_{1n'}}{N_0} \right) \left(\frac{h_{2n'}^2 p_{2n'} + h_{2n''}^2 p_{2n''}}{N_0} \right) \left(\frac{h_{3n''}^2 p_{3n''}}{N_0} \right) \right)^{\eta} \tag{A3}$$

For the CF-NOMA case, the sum rate maximization is obtained as follows.

$$\begin{aligned} \max_{p'_{1n'}, p'_{2n'}, p'_{2n''}, p'_{3n''}} \quad & \left(\left(\frac{h_{1n'}^2 p'_{1n'}}{N'_0} \right) \left(1 + \frac{h_{2n'}^2 p'_{2n'} + h_{2n''}^2 p'_{2n''}}{h_{2n'}^2 p'_{1n'} + N'_0} \right) \left(\frac{h_{3n''}^2 p'_{3n''}}{N'_0} \right) \right)^{\eta'} \\ \text{s.t.} \quad & p'_{1n'} + p'_{2n'} \leq P^{max} \\ & p'_{2n''} + p'_{3n''} \leq P^{max} \\ & p'_{2n'} - p'_{1n'} \geq \frac{P^{tol} N'_0}{h_{2n'}} \end{aligned} \tag{A4}$$

where $\eta' = B^{NOMA}/B = 1/2$, B^{NOMA} is the allocated bandwidth to each UE of the CF-NOMA cluster, $N'_0 = \delta N_0$ and $\delta = \frac{B/2}{B/3} = 1.5$. The objective function of (A4) can be written as (A5).

$$f'(\boldsymbol{p}') = \underbrace{\left(\left(\frac{h_{1n'}^2 p'_{1n'}}{N_0} \right) \left(\frac{h_{2n'}^2 P^{max} + h_{2n''}^2 p'_{2n''}}{N_0} \right) \left(\frac{h_{3n''}^2 p'_{3n''}}{N_0} \right) \right)^{\eta'}}_{f'_A(\boldsymbol{p}')} \left(\frac{N_0}{\delta^2 h_{2n'}^2 p'_{1n'}} \right)^{\eta'} \tag{A5}$$

First, we compare term in (A5) with $f(\boldsymbol{p})$. Considering the fact $\eta' > \eta$ and each term in the parentheses for $f'_A(\boldsymbol{p}')$ and $f(\boldsymbol{p})$ is greater than one, it can be seen that maximizing the NOMA objective $f'_A(\boldsymbol{p}')$ is similar to maximizing the OMA objective $f(\boldsymbol{p})$, having a larger bandwidth than that of the OMA (since $\eta' > \eta$), and at the same time $p_{2n'}$ is equal to the maximum allowed value P^{max}; this verifies the feasibility constraints of (A4). Therefore, by selecting suitable power levels, $f'_A(\boldsymbol{p}')$ will be greater than $f(\boldsymbol{p})$. One possible sub-optimal choice is to select $p'_{2n''} = 0$ and consequently $p'_{3n''} = P^{max}$. Therefore, considering the aforementioned sub-optimal values of $\boldsymbol{p}'$, and optimal values of $\boldsymbol{p}$, the ratio of $f'_A(\boldsymbol{p}')$ over $f(\boldsymbol{p})$ is always greater than or equal to (A6), expressed

in the following.

$$\left(\frac{1}{\delta^2 h_{2n'}^2 p'_{1n'}}\right)^{\eta'} \frac{(h_{1n'}^2 p'_{1n'} h_{2n'}^2 P^{max} h_{3n''}^2 P^{max})^{\eta'}}{(h_{1n'}^2 p_{1n'}(h_{2n'}^2 p_{2n'} + h_{2n''}^2 p_{2n''}) h_{3n''}^2 p_{3n''})^{\eta}} \tag{A6}$$

By simplifying (A6), and considering constraints (10), it can be verified that (A6) is higher than unity, and thus the superiority of CF-NOMA over CF-OMA is concluded. Considering that (10) is valid for all APs, if APs other than n' and n'' are added to G_1 and G_3, the terms added to the (A5) are correspondingly greater than those added to $f(\boldsymbol{p})$, and thus the outperformance of CF-NOMA over CF-OMA in cell-free NOMA networks is verified. ■

B) Proof of Theorem II: Similar to Theorem 1, first we consider that AP groups G_1 and G_3 consist of single APs denoted by n' and n'', and then extend the proof for groups containing multiple APs. The sum rate maximization problem for CF-NOMAC is formally written as follows.

$$\begin{aligned} \max_{p''_{1n'}, p''_{2n'}, p''_{2n''}, p''_{3n''}} \quad & \left(\frac{h_{1n'}^2 p''_{1n'}}{N''_0}\right)\left(\frac{h_{2n'}^2 p''_{2n'} + h_{2n''}^2 p''_{2n''}}{h_{2n'}^2 p''_{1n'} + h_{2n''}^2 p''_{3n''} + N''_0} + 1\right)\left(\frac{h_{3n''}^2 p''_{3n''}}{N''_0}\right)^{\eta''} \\ \text{s.t.} \quad & p''_{1n'} + p''_{2n'} \le P^{max} \\ & p''_{2n''} + p''_{3n''} \le P^{max} \\ & p''_{2n'} - p''_{1n'} \ge \frac{P^{tol} N''_0}{h_{2n'}^2} \\ & p''_{2n''} - p''_{3n''} \ge \frac{P^{tol} N''_0}{h_{2n''}^2} \end{aligned} \tag{A7}$$

where $\eta'' = B^{NOMAC}/B = 1$, B^{NOMAC} is the allocated bandwidth to each UE of the CF-NOMAC cluster and $N''_0 = 3N_0$. The objective function of (A7) is equal to (A8) in the following.

$$\begin{aligned} f''(\boldsymbol{p}'') = & \underbrace{\left(\left(\frac{h_{1n'}^2 p''_{1n'}}{N'_0}\right)\left(\frac{P^{max}(h_{2n'}^2 + h_{2n''}^2)}{N'_0}\right)\left(\frac{h_{3n''}^2 p''_{3n''}}{N'_0}\right)\right)^{\eta''}}_{f''_A(\boldsymbol{p}'')} \\ & \times \left(\frac{N'_0}{4(h_{2n'}^2 p''_{1n'} + h_{2n''}^2 p''_{3n''})}\right)^{\eta''} \end{aligned} \tag{A8}$$

Remember that the bandwidth allocated to each UE in CF-NOMA and CF-NOMAC clusters is $B/2$ and B respectively. First, we compare the term $f''_A(\boldsymbol{p}'')$ with $f'_A(\boldsymbol{p}')$. Noting that $\eta'' > \eta'$, and each term in the parentheses in both $f''_A(\boldsymbol{p}'')$ and $f'_A(\boldsymbol{p}')$ is greater than one, similar to the proof of Theorem 1, maximizing the term $f''_A(\boldsymbol{p}'')$ is similar to maximizing the sum rate of an OMA problem, having a larger bandwidth than that for $f'_A(\boldsymbol{p}')$ (since $\eta'' > \eta'$), and at the same time $p'_{2n''}$ is equal to the maximum allowed value P^{max}; this verifies the feasibility constraint, as well as the

power constraints of (A7). Therefore, it's concluded that by selecting suitable power values, $f''_A(\boldsymbol{p}'')$ will be greater than $f'_A(\boldsymbol{p}')$. The ratio of $f''(\boldsymbol{p}'')$ over $f'(\boldsymbol{p}')$, is obtained as follows:

$$\frac{h_{1n'}p''_{1n'}h_{3n''}p''_{3n''}(h^2_{2n'}+h^2_{2n''})P^{max}h_{2n'}N'_0N''^{-2}_0}{(h^2_{2n'}p''_{1n'}+h^2_{2n''}p''_{3n''})\sqrt{h^2_{2n'}p'_{2n'}+h^2_{2n''}p'_{2n''}}\sqrt{p'_{3n''}}} \tag{A9}$$

By simplifying (A9), we get (A10) as follows.

$$\left(\frac{h_{1n'}h_{3n''}P^{min}}{N''_0}\right)\left(\frac{h^2_{2n'}p^{max}}{N''_0}\right)\left(\frac{N'_0}{h^2_{2n'}p'_{2n'}+h^2_{2n''}p'_{2n''}}\times\frac{N'_0}{h^2_{2n'}p'_{3n''}}\right)^{\eta'} \tag{A10}$$

where $P^{min}=\min(p''_{1n'},p''_{3n''})$. It should be noted that the ratio (A10) with the optimal UEs power is always greater than or equal to (A9). The first two terms of (A10) are greater than the next two terms as they are associated with the SNRs of desired signals. On the other hand, the next two terms are associated with the SNRs of interference signals. By considering the high SNR assumption we conclude that the (A10) is greater than one. Considering that APs other than n' and n'' are added to G_1 and G_3, the terms added to the (A8) are correspondingly greater than those added to the objective function of (A7), and thus the outperformance of NOMAC over CF-NOMA in cell-free NOMA networks is verified. ■

Appendix B SIGNOMIAL PROGRAMMING

GP belongs to a class of nonlinear optimization techniques that possess numerous advantageous theoretical and computational properties [26]. Despite GP being seemingly non-convex in its standard form, it can be easily transformed into a convex optimization problem. GP can be represented in two interchangeable forms: the standard form and the convex form. The standard form involves constrained optimization of a specific function category known as a posynomial. The convex form is derived from the standard form by employing a logarithmic transformation of variables. The monomial function $f:\mathbb{R}^s_{++}\rightarrow\mathbb{R}$ is defined as follows:

$$f(p)=kp_1^{a^{(1)}}p_2^{a^{(2)}}\dots p_s^{a^{(J)}} \tag{B11}$$

where the multiplicative constant $d\geq 0$ and the exponential constants $a^{(j)}\in\mathbb{R}, j=1,2,...,J$. Sum of monomials, indexed by i, is called a posynomial that expressed in (B12).

$$f(p)=\sum_{i=1}^{I}k_ip_1^{a_i^{(1)}}p_2^{a_i^{(2)}}\dots p_s^{a_i^{(J)}} \tag{B12}$$

where $k_i\geq 0$, and the exponential constants $a_i^{(j)}\in\mathbb{R}, j=1,2,...,J,\ i=1,...,I$. The key features of a posynomial, are its positivity and convexity in the log domain. The

following optimization problem is called a GP problem in the standard form:

$$\begin{aligned} \min_{\boldsymbol{p}} \ & f_0(\boldsymbol{p}) \\ \text{s.t.} \ & f_s(\boldsymbol{p}) \leq 1, \quad s = 1, 2, ..., S \\ & h_v(\boldsymbol{p}) = 1, \quad v = 1, 2, ..., V \end{aligned} \tag{B13}$$

where f_s and h_v are posynomial and monomial, respectively. Although the posynomial seems to be a non-convex function, it becomes a convex function after using the $log - sum - exp$ transformation In contrast to the constrained or unconstrained minimization of polynomials, the minimization of a posynomial within GP relaxation loosens the integer constraint on the exponential constants while enforcing a positive constraint on the multiplicative constants and variables. These two problems exhibit a distinct disparity: polynomial minimization is known to be NP-hard, whereas GP can be transformed into convex optimization using polynomial-time algorithms with guaranteed global optimally. GP in the standard form allows only the upper bound inequality constraints for posynomials and equality constraints for monomials. However, these requirements might be violated in practice. i.e. there might exist lower-bounded posynomial inequality constraints, as well as equality constraints having posynomials.This issue can be tackled by extending GP to signomial programming (SP): minimizing a signomial objective function subject to upper bounded inequality constraints on signomials, and/or equality constraints on posynomials. A signomial function which is expressed as (B14) is a sum of monomials, wherein, the coefficient of each monomial can be positive or negative.

$$f_s(p) = \sum_{i=1}^{I} c_i \prod_{j=1}^{J} p_j^{a_i^{(j)}}, \quad s = 1, ..., S \tag{B14}$$

where $c_i \in \mathbb{R}, a_i^{(j)} \in \mathbb{R}, \ \forall e, j, \ \boldsymbol{p} \in \mathbb{R}_{++}^{J}$. SP is an extension of the GP problem, which cannot be generally turned into a convex problem [26]. Complementary GP is an approach for solving SP problems. This approach allows upper bound constraints on the ratio between two posynomials and then applies a monomial approximation iteratively. This is called the condensation technique, which is an instance of the cutting-plane method for nonlinear programming. The conversion from an SP into a Complementary GP is trivial. An inequality in SP is in the form of (B15).

$$f_{s1}(p) - f_{s2}(p) \leq 1 \tag{B15}$$

where $f_{s1}(p)$ and $f_{s2}(p)$ are posynomials. (B15) is equivalent to the following inequality.

$$\frac{f_{s1}(p)}{1 + f_{s2}(p)} \leq 1 \tag{B16}$$

There exist two options for making the monomial approximation. One is to approximate the denominator $1+f_{s2}(p)$ with a monomial but leave the numerator $f_{s1}(p)$ as a posynomial. This is called the single condensation method, and results in a GP approximation of a SP. An alternate option is to employ the monomial approximation for both the denominator and numerator, commonly referred to as the double condensation approach. The double condensation approach entails a higher degree of computational complexity. Therefore, in this paper, we exclusively utilize the single condensation approach and incorporate the monomial approximation for enhanced precision. In the context of single condensation, we employ a simplified approximation built upon the geometric inequality concept, which has consequently fostered the evolution of GP. The following inequality forms an upper-bound monomial approximation.

$$\sum_i \alpha_i \nu_i \ \geq \ \prod_i \nu_i^{\alpha_i} \tag{B17}$$

where $\nu_i > 0$, $\alpha_i > 0, \forall i$, $\sum_i \alpha_i = 1$. Letting $u_i = \alpha_i \nu_i$, (B17) can be written as follows:

$$\sum_i u_i \ \geq \ \prod_i (\frac{u_i}{\alpha_i})^{\alpha_i} \tag{B18}$$

Let $u_i(\boldsymbol{p})$ be the monomial term in posynomial $f(\boldsymbol{p}) = \sum_i u_i(\boldsymbol{p})$. This approximation is in the conservative direction because the original constraint is tightened. One possible choice for α is

$$\alpha_i(\boldsymbol{p}) = \frac{u_i(\boldsymbol{p})}{f(\boldsymbol{p})}, \qquad \forall i \tag{B19}$$

Given an α for each lower bound posynomial inequality, a standard form GP can be obtained based on the above monomial approximation of the SP. It should be noted that both the monomial approximation and the aforementioned selection of α might not yield the optimal approximation, either in terms of minimizing the approximation error or enabling the computation of a global optimizer for the original SP. To mitigate this limitation, an iterative procedure can be employed to solve the geometric mean approximation of the SP. This iterative process involves initiating with some feasible power vector $\boldsymbol{p}^v$ and subsequently computing $\alpha(p^v)$. This leads to the formation of a GP problem which yields the power $\boldsymbol{p}^{v+1}$. The algorithm continues until it converges to a fixed point.

References

[1] H. A. Ammar, R. Adve, S. Shahbazpanahi, G. Boudreau and K. V. Srinivas, "User-Centric Cell-free massive MIMO networks: A survey of opportunities, challenges and solutions," in IEEE Communications Surveys & Tutorials, vol. 24, no. 1, pp. 611-652, First quarter 2022.

[2] Z. Ding, P. Fan, and H. V. Poor, "Impact of user pairing on 5G nonorthogonal multiple-access downlink transmissions," IEEE Trans. Veh.Technol., vol. 85, no. 5, pp. 6010–6023, Aug. 2016.

[3] Özlem Tugfe Demir, Emil Björnson, Luca Sanguinetti, "Foundations of User-Centric Cell-Free Massive MIMO,". 2021.

[4] M. S. Ali, H. Tabassum, and E. Hossain, "Dynamic user clustering and power allocation for uplink and downlink non-orthogonal multiple access (NOMA) systems," in IEEE Access, vol. 4, pp. 6325-6343, 2016.

[5] M. Monemi, H. Tabassum and R. Zahedi, "On the performance of non-orthogonal multiple access (NOMA): terrestrial vs. aerial Networks," 2020 IEEE Eighth International Conference on Communications and Networking (ComNet), Hammamet, Tunisia, 2020.

[6] X. Zhang and Q. Zhu, "NOMA and User-Centric based cell-free massive MIMO over 6G big-data mobile wireless networks," GLOBECOM 2020 - 2020 IEEE Global Communications Conference, Taipei, Taiwan, 2020.

[7] Z. Wang, D. Zhang, K. Xu, W. Xie, J. Xv, and X. Li, "NOMA in cell-free mMIMO systems with AP selection," 2020 International Conference on Wireless Communications and Signal Processing (WCSP), Nanjing, China, 2020.

[8] Q. Gao, M. Jia, Q. Guo, X. Gu, and L. Hanzo, "Jointly optimized beamforming and power allocation for full-duplex cell-free NOMA in space-ground integrated networks," in IEEE Transactions on Communications, vol. 71, no. 5, pp. 2816-2830, May 2023.

[9] J. Zhang, J. Fan, J. Zhang, D. W. K. Ng, Q. Sun and B. Ai, "Performance analysis and optimization of NOMA-based cell-free massive MIMO for IoT," in IEEE Internet of Things Journal, vol. 9, no. 12, pp. 9625-9639, 15 June 15, 2022.

[10] R. Sayyari, J. Pourrostam and M. J. M. Niya, "Cell-free massive MIMO system with an adaptive switching algorithm between cooperative NOMA, non-cooperative NOMA, and OMA modes," in IEEE Access, vol. 9, pp. 149227-149239, 2021.

[11] M. Bashar, K. Cumanan, A. G. Burr, H. Q. Ngo, L. Hanzo and P. Xiao, "On the performance of cell-free massive MIMO relying on adaptive NOMA/OMA mode-switching," in IEEE Transactions on Communications, vol. 68, no. 2, pp. 792-810, Feb. 2020.

[12] A. Chowdary, G. Chopra, A. Kumar, and L. R. Cenkeramaddi, "Enhanced user grouping and pairing scheme for CoMP-NOMA-based cellular networks," 2022 14th International Conference on COMmunication Systems & NETworks (COMSNETS), Bangalore, India, 2022.

[13] M. S. Ali, E. Hossain, A. Al-Dweik and D. I. Kim, "Downlink power allocation for CoMP-NOMA in multi-cell networks," in IEEE Transactions on Communications, vol. 66, no. 9, pp. 3982-3998, Sept. 2018.

[14] A. J. Muhammed et al., "Resource allocation for energy-efficient NOMA system in coordinated multi-point networks," in IEEE Transactions on Vehicular Technology, vol. 70, no. 2, pp. 1577-1591, Feb. 2021.

[15] Y. Dai, J. Liu, M. Sheng, N. Cheng, and X. Shen, "Joint optimization of BS clustering and power control for NOMA-enabled CoMP transmission in dense cellular networks," in IEEE Transactions on Vehicular Technology, vol. 70, no. 2, pp. 1924-1937, Feb. 2021.

[16] M. Hedayati and I. M. Kim, "CoMP-NOMA in the SWIPT networks," in IEEE Transactions on Wireless Communications, vol. 19, no. 7, pp. 4549-4562, July 2020.

[17] M. Elhattab, M. A. Arfaoui, and C. Assi, "Joint clustering and power allocation in coordinated multipoint assisted C-NOMA cellular networks," in IEEE Transactions on Communications, vol. 70, no. 5, pp. 3483-3498, May 2022.

[18] M. Bashar, K. Cumanan, A. G. Burr, H. Q. Ngo, L. Hanzo and P. Xiao, "On the Performance of Cell-Free Massive MIMO Relying on Adaptive NOMA/OMA Mode-Switching," in IEEE Transactions on Communications, vol. 68, no. 2, pp. 792-810, Feb. 2020.

[19] T. K. Nguyen, H. H. Nguyen, and H. D. Tuan, "Max-Min QoS power control in generalized cell-free massive MIMO-NOMA with optimal backhaul combining," in IEEE Transactions on Vehicular Technology, vol. 69, no. 10, pp. 10949-10964, Oct. 2020.

[20] Q. Gao, M. Jia, Q. Guo, X. Gu, and L. Hanzo, "Jointly optimized beamforming and power allocation for full-duplex cell-free NOMA in space-ground integrated networks," in IEEE Transactions on Communications, vol. 71, no. 5, pp. 2816-2830, May 2023.

[21] Y. Li and G. A. Aruma Baduge, "NOMA-aided cell-free massive MIMO systems," in IEEE Wireless Communications Letters, vol. 7, no. 6, pp. 950-953, Dec. 2018.

[22] W. Zhao, H. Wang and R. Song, "Two user clustering schemes for cell-free massive MIMO-NOMA system," 2021 13th International Conference on Wireless Communications and Signal Processing (WCSP), Changsha, China, 2021.

[23] Q. N. Le, V. -D. Nguyen, O. A. Dobre, N. -P. Nguyen, R. Zhao, and S. Chatzinotas, "Learning-assisted user clustering in cell-free massive MIMO-NOMA networks," in IEEE Transactions on Vehicular Technology, vol. 70, no. 12, pp. 12872-12887, Dec. 2021.

[24] X. -T. Dang, M. T. P. Le, H. V. Nguyen, S. Chatzinotas and O. -S. Shin, "Optimal user pairing approach for NOMA-based cell-free massive MIMO systems," in IEEE Transactions on Vehicular Technology, vol. 72, no. 4, pp. 4751-4765, April 2023.

[25] H. Q. Ngo, A. Ashikhmin, H. Yang, E. G. Larsson, and T. L. Marzetta, "Cell-free massive MIMO versus small cells," IEEE Trans. Wireless Commun., vol. 16, no. 3, pp. 1834–1850, Mar. 2017.

[26] Mung Chiang, "Geometric programming for communication systems," Now Foundations and Trends, 2005.

[27] S. Boyd and L. Vandenberghe, "Convex Optimization". Cambridge University Press, 2004